

Thermal conductivity and specific heat capacity measurements of CuO nanofluids

Benigno Barbés · Ricardo Páramo ·
Eduardo Blanco · Carlos Casanova

Received: 12 April 2013 / Accepted: 5 November 2013 / Published online: 26 November 2013
© Akadémiai Kiadó, Budapest, Hungary 2013

Abstract A study of thermal properties of CuO dispersed in water and ethylene glycol as a function of the particle volume fraction and at temperatures between 298 and 338 K has been performed. Thermal conductivities have been studied by the steady-state coaxial cylinders method, using a C80D microcalorimeter (Setaram, France) equipped with special calorimetric vessels. Heat capacities have been measured with a Micro DSC II microcalorimeter (Setaram, France) with batch cells designed in our laboratory and the “scanning or continuous method.” Results for thermal conductivities can be well justified using a classical model (Hamilton–Crosser), and experimental measurements of heat capacities can be justified with a model of particles in thermal equilibrium with the base fluid.

Keywords Thermal conductivity · Specific heat capacity · Nanofluid · Coaxial cylinder method · Microcalorimeter

Introduction

The number of important and continuous advances in nanotechnology during the last years have led to the emergence of a new generation of heat transfer fluids called nanofluids, in which nanometer-sized particles with high thermal conductivity are dispersed and suspended in a base

liquid. Nanofluids have great potential to improve the heat transfer and energy efficiency in a variety of applications. Thermal properties of nanofluids, including thermal conductivity, viscosity, specific heat capacity, convective heat transfer coefficient, and critical heat flux have been extensively studied [1–31].

One of the most outstanding features of nanofluids is the increase in thermal conductivity compared to that of the base fluid, even in the case of very small particle volume fractions. Experimental studies show that thermal conductivity of nanofluids depends on many factors such as particle material, particle size and shape, particle volume fraction, agglomeration of particles, base fluid material, pH value, temperature, and additives.

There are two kinds of methods for thermal conductivity measurement [32], namely transient and steady state. We performed our measurements with the steady-state coaxial cylinders method, using a Setaram C80D microcalorimeter equipped with calorimetric vessels, also developed by Setaram, suitable for thermal conductivities of liquids. This method has the drawback that it is time consuming, though it permits a good temperature control and a very accurate measurement of the heat flow which passes through the sample; this is the key measurement that, with a good calibration method, gets accurate and reliable experimental thermal conductivity data. This method is particularly suitable for studying nanofluids because the measurement is made with very small temperature gradients and with practical absence of natural convection [33].

General measurements of thermal conductivity are often characterized by poor reproducibility and errors of about 2–5 % [34–36]. Specifically in the case of nanofluids, there are large discrepancies and inconsistencies in bibliography, showing the complexity of the thermal transport mechanism in this type of fluids. Identical samples being measured with

B. Barbés · R. Páramo · C. Casanova (✉)
Departamento de Física Aplicada, Universidad de Valladolid,
47011 Valladolid, Spain
e-mail: casanova@termo.uva.es

E. Blanco
Área de Mecánica de Fluidos, Universidad de Oviedo,
33271 Gijón, Spain

different methods usually result in large differences among values [37]. The main source of discrepancies seems to be the particles and conglomerates size distribution, which depends largely on the way the nanofluids are made. In this work, nanofluids were prepared by a well-established two-step method [38] and the nanoparticle size distribution was measured using a light scattering technique.

The specific heat basically represents the thermal storage capacity of a system, but it is also useful to calculate other related quantities like dynamic thermal conductivity and diffusivity. Furthermore, it is a key property for describing the heat transfer performance of flowing nanofluids in terms of the convective heat transfer coefficient and the Nusselt number. Research work on the specific heat capacity at constant pressure, c_p , of nanofluids is limited [39–52] compared to other properties such as thermal conductivity and viscosity. It depends on the specific heat capacity of nanoparticles and base fluid, particle volume fraction, and temperature. In order to measure the specific heat capacity of nanoparticles and nanofluids, we used a Setaram Micro DSC II microcalorimeter which provides very accurate values of specific heat capacity.

This paper presents thermal conductivity and specific heat capacity measurements of nanoparticles of CuO dispersed in water and ethylene glycol (EG) as a function of the particle volume concentration, at temperatures between 298 and 338 K. Some molecular theories on heat transfer in nanofluids applied to our systems are also discussed.

Experimental

The nanoparticles used in this work were CuO (NanoArk[®], 97.5 %, 23–37 nm APS powder) supplied by Alfa Aesar. Bi-distilled and deionised water and ethylene glycol (Fluka, puriss. p.a. ≥ 99.5 %) were used as the base fluids. The nanoparticle volume fractions of nanofluids were calculated from the masses of nanoparticles powder, using the true density provided by the supplier ($6,500 \text{ kg m}^{-3}$), and that of the base fluid. A two-step method was used to prepare the nanofluids. Nanoparticles were first dispersed into the base fluid in a flask of 30 mL, approximately, and the mixture was dispersed ultrasonically using a tip sonicator (Hielscher UP100H) for 1 h at a power of 60 W, to break up the agglomerates. Nanofluids made up following this protocol were found to be appropriate to obtain reliable thermal conductivity and specific heat capacity measurements, with good repeatability during long periods of time. An increase of the sonication time did not improve the results. These facts were confirmed by light scattering measurements using a Malvern AutoSizer Lo-C for particle size measurements (Malvern Instruments Ltd., UK). Copper oxide nanoparticles size distributions in water are

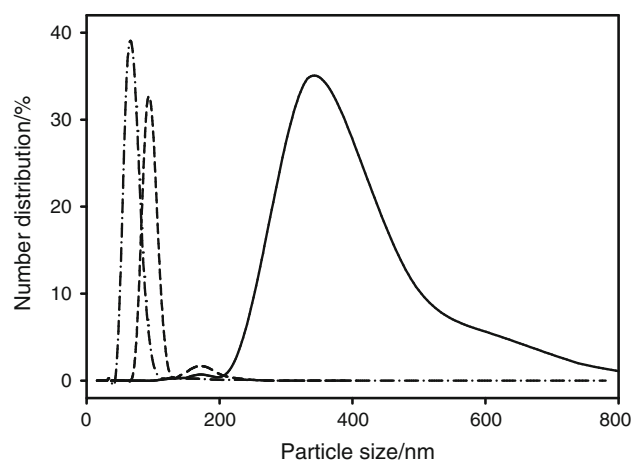


Fig. 1 Nanoparticles size distribution for water containing 1 vol% CuO. Without sonication (*thick line*), at 1st day (*dashed line*) and at 4th day (*dashed–dotted line*)

presented in Fig. 1. They show that the sonication process is very effective for removing larger aggregates and narrowing the main peak. Furthermore, it can be seen that the size distributions do not vary significantly over several days. Similar behavior is found for EG nanofluids.

The method for measuring thermal conductivities k , using a differential heat-flow microcalorimeter C80D provided with a set of vessels from Setaram (France), was described in detail elsewhere [33, 38]. It can be obtained as a function of the calorimeter signal $\Delta\dot{Q}$, by the expression:

$$k = \frac{A - \Delta\dot{Q}}{B \times \Delta\dot{Q} + C} \quad (1)$$

where the constants A , B , and C depend on the thermal response of the calorimeter components with temperature [53], but not on the liquid measured. A suitable calibration was performed, using three liquids of well-known thermal conductivity: distilled and deionised water [35, 54], glycerol anhydrous (Fluka ≥ 99.5 %) [34], and n -heptane (Fluka, ≥ 99.5 %) [35, 55]. Overall uncertainty in thermal conductivity is about 1.5 % [33].

In order to measure the specific heat capacity of nanoparticles and nanofluids, a Setaram Micro DSC II microcalorimeter provided with “batch” vessels designed in our laboratory, was used. The method was also described in a previous work [38], and measurements have a relative uncertainty of 0.3 % [56].

Results and discussion

Thermal conductivity measurements

Experimental values of the thermal conductivity as a function of temperature and nanoparticle volume fraction

Table 1 Experimental thermal conductivity of CuO/water nanofluid as a function of the temperature and nanoparticle volume fraction

$\phi/\%$	$k/\text{J m}^{-1} \text{K}^{-1}$				
	298.15 K	308.15 K	318.15 K	328.15 K	338.15 K
0.4	0.6233	0.6380	0.6513	0.6621	0.6720
0.7	0.6293	0.6443	0.6569	0.6669	0.6778
1.0	0.6382	0.6547	0.6650	0.6753	0.6839
1.5	0.6462	0.6623	0.6768	0.6872	0.6972

Table 2 Experimental thermal conductivity of CuO/EG nanofluid as a function of the temperature and nanoparticle volume fraction

$\phi/\%$	$k/\text{J m}^{-1} \text{K}^{-1}$				
	298.15 K	308.15 K	318.15 K	328.15 K	338.15 K
0.4	0.2549	0.2565	0.2583	0.2602	0.2623
0.7	0.2598	0.2616	0.2637	0.2657	0.2679
1.5	0.2661	0.2687	0.2704	0.2731	0.2765
3.0	0.2794	0.2828	0.2855	0.2890	0.2925

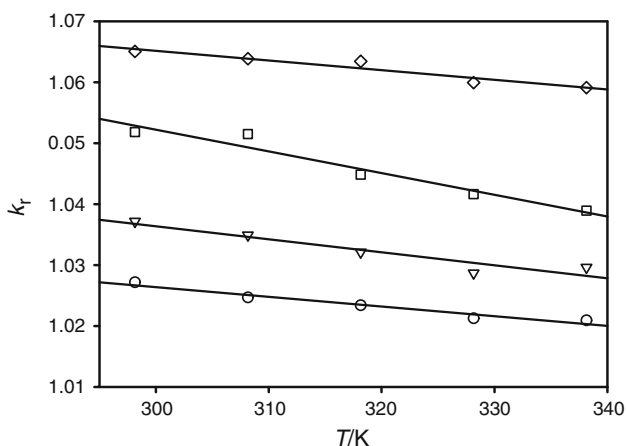


Fig. 2 Relative thermal conductivity of CuO/water nanofluid versus temperature, at several volume fractions (circles 0.4 %, inverted triangles 0.7 %, squares 1 %, diamonds 1.5 %). Full lines (linear correlations) are intended to guide the eyes

(ϕ) of CuO/water and CuO/EG nanofluids are presented in Tables 1 and 2, respectively. Figures 2 and 3 show the relative thermal conductivity k_r , (ratio of the thermal conductivity of the nanofluid with respect to that of the base fluid) as a function of the temperature and volume fraction at 298.15 and 338.15 K for the CuO/water nanofluid. Figures 3 and 4 depict the same information for the CuO/EG nanofluid. The thermal conductivity data of water [35, 54] and ethylene glycol [34] were taken from the literature.

Figures 5 and 6 compare our results of k_r , as a function of the particle volume concentration at 298.15 K for the

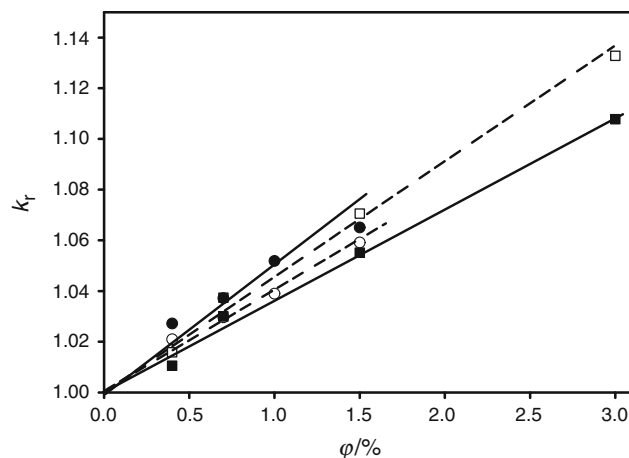


Fig. 3 Relative thermal conductivity of CuO/water (filled circles 298.15, open circles 338.15) and CuO/EG (filled squares 298.15, open squares 338.15) nanofluids versus volume fraction at 298.15 and 338.15 K. Full lines (correlations) are intended to guide the eyes

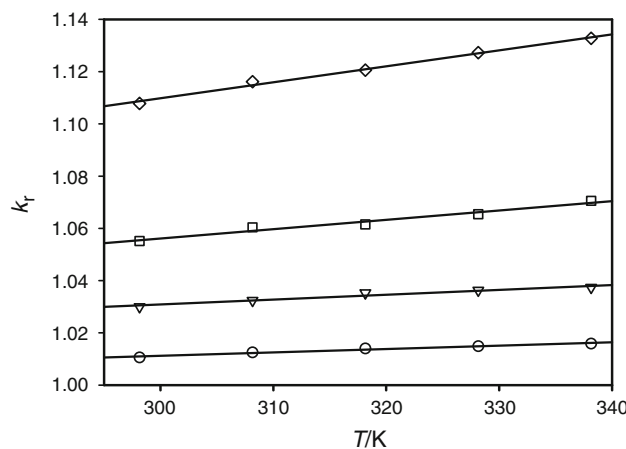


Fig. 4 Relative thermal conductivity of CuO/EG nanofluid versus temperature, at several volume fractions (circles 0.4 %, inverted triangles 0.7 %, squares 1.5 %, diamonds 3 %). Full lines (linear correlations) are intended to guide the eyes

CuO/water and CuO/EG nanofluids, with recent published data for the same nanofluids in similar conditions (nanoparticle size and temperature), along with the reported uncertainties. A large degree of randomness and scatter were observed in the literature data; in any case, the results of the present paper are within the general range of values obtained from various sources. The scatter of the experimental data could possibly be attributed to several factors including nanofluid manufacturing process, particle size, and clustering, as well as the thermal conductivity experimental technique. The two-step method with sonication used in this work has been shown to be suitable to obtain a stable nanofluid over long periods and with an appropriate size distribution. Furthermore, the microcalorimetric technique ensures that our thermal conductivity measurements

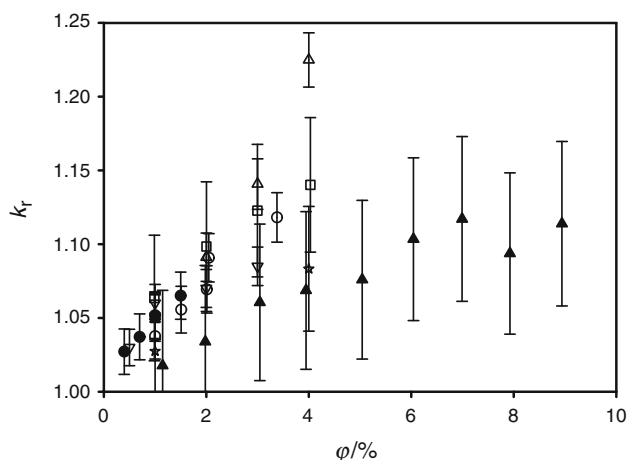


Fig. 5 Relative thermal conductivity of CuO/water nanofluid versus volume fraction: Present work (filled circles, 23–37 nm, 298 K), Lee et al. [57] (open circles, 24 nm, 298 K), Eastman et al. [58] (open triangles, 24 nm, 298 K), Das et al. [59] (open squares, 29 nm, 294 K), Patel et al. [60] (open inverted triangles, 31 nm, 293 K), Zhang et al. [61] (open stars, 32 nm, 296 K), Mintsa et al. [62] (filled triangles, 29 nm, 298 K), Hwang et al. [63] (filled squares, 22 nm, 298 K)

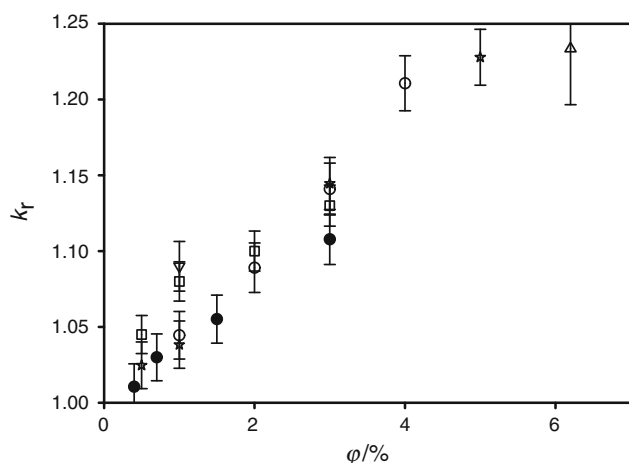


Fig. 6 Relative thermal conductivity of CuO/EG nanofluid versus volume fraction: present work (filled circles, 23–37 nm, 298 K), Lee et al. [57] (open circles, 24 nm, 298), Wang et al. [64] (open triangles, 23 nm, 298 K), Patel et al. [60] (open squares, 31 nm, 293 K), Hwang et al. [63] (open inverted triangles, 33 nm, 298 K), Gowda et al. [6] (open stars, 30 nm, 297 K)

are performed at a constant temperature and with practical absence of natural convection, as has been justified elsewhere [33]. These facts make us confident that our measurements are correct. They represent a relevant contribution to the issue of scatter of data as they have been obtained with a technique that eliminates possible sources of error (high temperature gradients and convection). The relative thermal conductivity increases almost linearly with concentration. For the CuO/water and CuO/EG nanofluids, the thermal conductivity increments observed in this paper

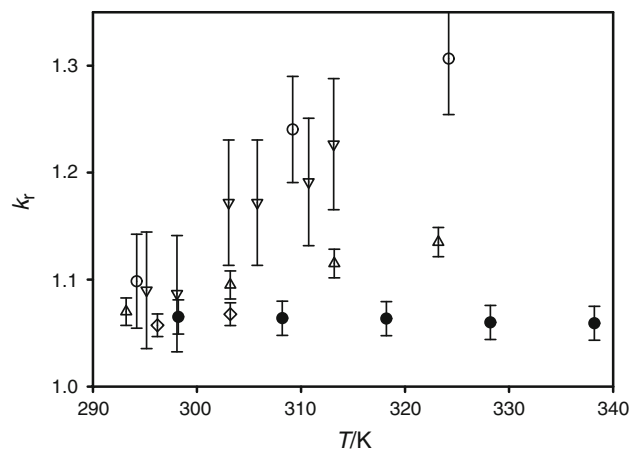


Fig. 7 Relative thermal conductivity of CuO/water nanofluid versus temperature: present work (filled circles, 23–37 nm, 1.5 %), Das et al. [59] (open circles, 29 nm, 2 %), Patel et al. [60] (open triangles, 31 nm, 1.2 %), Zhang et al. [61] (open diamonds, 33 nm, 2.6 %), Mintsa et al. [62] (open inverted triangles, 29 nm, 3.3 %)

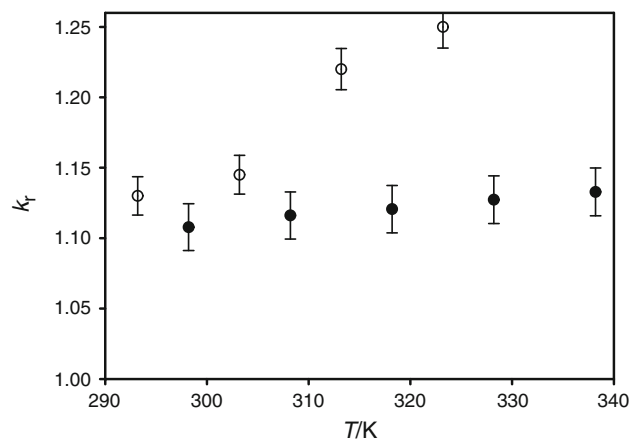


Fig. 8 Relative thermal conductivity of CuO/EG nanofluid versus temperature: Present work (filled circles, 23–37 nm, 3 %), Patel et al. [60] (open circles, 31 nm, 3 %)

are in good agreement with the literature values within the reported uncertainties, except with data from [62].

Figures 7 and 8 compare our experimental results of k_r as a function of the temperature for the CuO/water (1.5 vol%) and CuO/EG (3.0 vol%) nanofluids, with recently published data for the same nanofluids in similar conditions (nanoparticle size and concentration), along with the reported uncertainties. In the scarce literature data available, it is shown that the relative thermal conductivity increases with temperature; nevertheless, our measurements indicate that it is essentially temperature independent. The same behavior is found in Al_2O_3 nanofluids made with the same base fluid [38, 65] and in CuO with diathermic oil nanofluids [29]. We conclude that the observed growth of the thermal conductivity of our nanofluids with increasing temperature is due mainly to the base fluids (water and ethylene glycol) rather

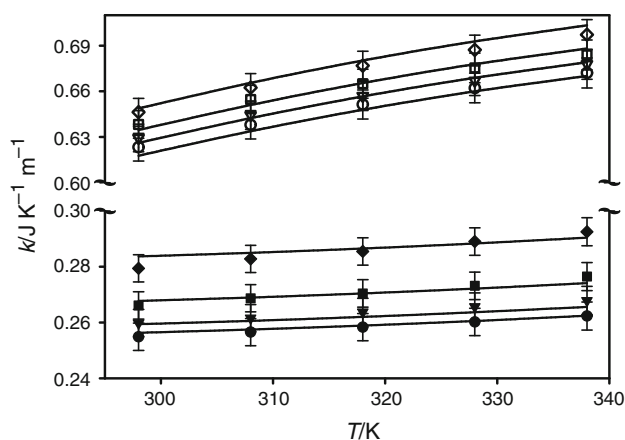


Fig. 9 Thermal conductivity of CuO/water nanofluids at different nanoparticle volume fractions (*open circles* 0.4 %, *open inverted triangles* 0.7 %, *open squares* 1.0 %, *open diamonds* 1.5 %); and CuO/EG nanofluid at different nanoparticle volume fractions (*filled circles* 0.4 %, *filled inverted triangles* 0.7 %, *filled squares* 1.5 %, *filled diamonds* 3 %) in function of temperature. *Full lines* represent the predictions of the Hamilton–Crosser model

than to the nanoparticles and, therefore, that the thermal conductivity enhancement is temperature independent.

Figure 9 compares the measurements of this work with those calculated with the Hamilton and Crosser [66] model, an extension of Maxwell model [67] (low-concentration diffusion of identical solid spheres in a liquid) to apply it to non-spherical particles. They show good agreement. We have also analyzed the predictions of other models such as that of Nan et al. [68], which take into account the Kapitza thermal contact resistance or the more complex model of Jang et al. [69], which also includes the effect of Brownian motion of nanoparticles at the molecular and nanoscale level. The improvements obtained with these models are in all cases within the experimental error range. It can be concluded that the experimental thermal conductivities of the nanofluids studied in this work can be properly justified using a simple classical model and that no anomalous enhancement of thermal conductivity was observed [37, 61, 70].

Specific heat capacity measurements

Experimental values of the specific heat capacities of CuO nanoparticles and nanofluids obtained with water and EG as base fluids as a function of the particle volume concentration and at temperatures between 298 and 338 K are presented in Tables 3 and 4. All these data fit nicely by a linear curve-fit:

$$c_p = a + b \times T \tag{2}$$

Table 5 shows the coefficients of linear regressions with their standard errors and the root-mean-square deviations of the fits.

Table 3 Experimental specific heat capacities of CuO nanoparticles and CuO/water nanofluid as a function of the temperature and nanoparticle volume fraction

T/K	$c_p / \text{J K}^{-1} \text{g}^{-1}$	T/K	$c_p / \text{J K}^{-1} \text{g}^{-1}$	T/K	$c_p / \text{J K}^{-1} \text{g}^{-1}$
CuO nanoparticles		0.4 %		0.7 %	
296.28	0.536	298.31	4.082	298.31	4.018
298.30	0.535	300.32	4.081	300.32	4.015
300.32	0.533	302.35	4.079	302.34	4.013
302.84	0.538	304.36	4.082	304.36	4.015
304.85	0.548	306.37	4.085	306.37	4.021
306.86	0.551	308.38	4.085	308.37	4.023
308.87	0.555	310.38	4.082	310.38	4.019
310.88	0.561	312.39	4.082	312.39	4.018
312.89	0.560	314.40	4.084	314.40	4.019
315.40	0.563	316.41	4.085	316.40	4.020
317.40	0.566	318.42	4.084	318.41	4.021
319.40	0.570	320.42	4.084	320.41	4.022
321.40	0.575	322.42	4.086	322.41	4.023
323.40	0.576	324.42	4.087	324.41	4.023
325.40	0.576	325.92	4.088	325.91	4.024
327.40	0.580	327.92	4.089	327.92	4.026
329.41	0.584	329.92	4.089	329.92	4.028
331.41	0.582	331.92	4.090	331.92	4.029
333.40	0.585	333.91	4.090	333.91	4.030
335.39	0.588	335.90	4.092	335.90	4.031
337.38	0.597	337.89	4.094	337.89	4.035
1.0 %		1.5 %		2.0 %	
298.31	3.956	298.30	3.855	298.30	3.753
300.33	3.954	300.33	3.853	300.32	3.751
302.34	3.952	302.34	3.850	302.34	3.748
304.36	3.953	304.36	3.851	304.35	3.749
306.37	3.958	306.37	3.857	306.36	3.755
308.37	3.962	308.37	3.861	308.37	3.760
310.38	3.959	310.38	3.858	310.38	3.758
312.39	3.957	312.39	3.856	312.39	3.754
314.40	3.958	314.40	3.857	314.39	3.755
316.42	3.959	316.41	3.858	316.40	3.757
318.41	3.958	318.41	3.858	318.40	3.757
320.41	3.959	320.41	3.859	320.40	3.758
322.42	3.960	322.41	3.860	322.41	3.758
324.42	3.961	324.41	3.861	324.41	3.759
325.92	3.962	325.92	3.861	325.91	3.760
327.92	3.963	327.91	3.863	327.91	3.761
329.92	3.964	329.92	3.864	329.91	3.762
331.91	3.965	331.91	3.865	331.91	3.763
333.91	3.965	333.90	3.866	333.90	3.764
335.90	3.966	335.89	3.867	335.89	3.765
337.88	3.967	337.88	3.869	337.87	3.768

Table 4 Experimental specific heat capacities of CuO/EG nanofluid as a function of the temperature and nanoparticle volume fraction

T/K	$c_p/J\ K^{-1}\ g^{-1}$	T/K	$c_p/J\ K^{-1}\ g^{-1}$	T/K	$c_p/J\ K^{-1}\ g^{-1}$	T/K	$c_p/J\ K^{-1}\ g^{-1}$
0.4 %		0.7 %		1.5 %		3.0 %	
296.33	2.358	296.31	2.330	296.31	2.260	296.31	2.127
298.34	2.369	298.33	2.340	298.33	2.270	298.32	2.136
300.36	2.379	300.35	2.349	300.35	2.280	300.34	2.145
302.88	2.390	302.87	2.361	302.87	2.291	302.86	2.156
304.90	2.402	304.89	2.372	304.88	2.302	304.88	2.167
306.91	2.412	306.90	2.382	306.89	2.311	306.89	2.176
308.91	2.422	308.91	2.391	308.90	2.321	308.89	2.185
310.93	2.432	310.92	2.401	310.91	2.330	310.91	2.194
312.93	2.444	312.93	2.412	312.92	2.341	312.91	2.205
315.45	2.456	315.44	2.425	315.43	2.353	315.43	2.217
317.46	2.467	317.44	2.436	317.43	2.363	317.43	2.226
319.45	2.477	319.44	2.445	319.44	2.372	319.43	2.236
321.45	2.488	321.45	2.456	321.44	2.383	321.43	2.247
323.46	2.499	323.45	2.467	323.44	2.393	323.43	2.258
325.46	2.512	325.45	2.479	325.44	2.405	325.43	2.270
327.96	2.524	327.95	2.491	327.94	2.417	327.93	2.283
329.96	2.535	329.95	2.502	329.94	2.428	329.94	2.295
331.95	2.547	331.95	2.513	331.93	2.439	331.93	2.307
333.95	2.558	333.94	2.524	333.92	2.451	333.92	2.319
335.94	2.570	335.93	2.535	335.92	2.464	335.91	2.333
337.43	2.580	337.42	2.546	337.41	2.476	337.40	2.345

Table 5 Coefficients of Eq. (2) and root-mean-square deviations

$\varphi/\%$	$a \pm \sigma_a /$ $J\ K^{-1}\ g^{-1}$	$10^4(b \pm \sigma_b) /$ $J\ K^{-2}\ g^{-1}$	$\sigma / J\ K^{-1}\ g^{-1}$
CuO/water			
CuO nanoparticles			
0.4	0.10 ± 0.02	14.7 ± 0.6	0.003
0.7	3.99 ± 0.01	2.9 ± 0.3	0.001
1.0	3.89 ± 0.01	4.1 ± 0.4	0.002
1.5	3.86 ± 0.01	3.0 ± 0.4	0.002
2.0	3.74 ± 0.01	3.8 ± 0.4	0.002
CuO/EG			
0.4	0.770 ± 0.010	53.5 ± 0.3	0.002
0.7	0.779 ± 0.010	52.2 ± 0.3	0.002
1.5	0.738 ± 0.016	51.3 ± 0.5	0.003
3.0	0.583 ± 0.024	51.9 ± 0.8	0.004

In the literature, there are very few reliable data on specific heat capacities of water- or EG-based CuO nanofluids to compare with. Zhou et al. [44] have studied the specific heat capacities of EG-based CuO nanofluid at room temperature as a function of the nanoparticle volume fraction. Pantzani et al. [46] have measured the specific

heat capacities of water-based CuO nanofluids at 298 K and three-particle volume fraction with a microcalorimeter. Recently, O'Hanley et al. [40] have measured the specific heat capacities of water-based CuO nanofluids at 308, 318, and 328 K and various nanoparticle concentrations using a heat-flux type differential scanning calorimeter. It is worth noting that our results are in excellent agreement with those measurements within the experimental error range.

Assuming that the nanoparticles and the base fluid are in thermal equilibrium, the specific heat capacity of nanofluid can easily be deduced on the basis of the First Law of Thermodynamics. As has been explained previously [38], the specific heat capacity of nanofluid $c_{p,nf}$ is related to the specific heat capacities of nanoparticles $c_{p,np}$ and base fluid $c_{p,bf}$ by:

$$c_{p,nf} = \frac{\varphi \cdot \rho_{np} \cdot c_{p,np} + (1 - \varphi) \cdot \rho_{bf} \cdot c_{p,bf}}{\varphi \cdot \rho_{np} + (1 - \varphi) \cdot \rho_{bf}} \quad (3)$$

where ρ_{nf} , ρ_{np} , and ρ_{bf} are the densities of the nanofluid, nanoparticles, and base fluid, respectively, and φ is the nanoparticle volume fraction.

Figure 10 shows a comparison of our experimental results of the specific heat capacities at 303 and 333 K as a function of the volume fraction concentration for the CuO/

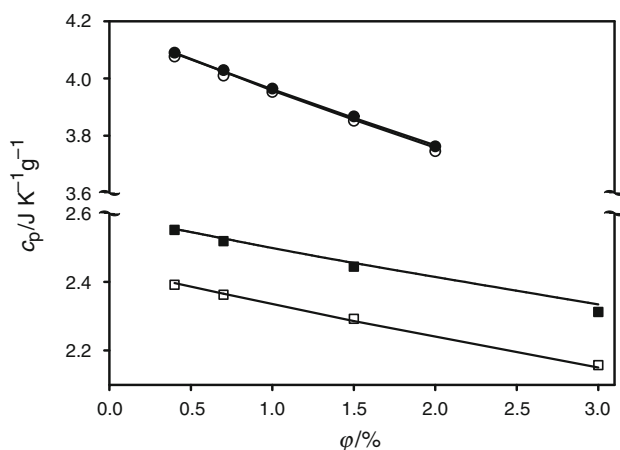


Fig. 10 Specific heat capacity of CuO/water nanofluid versus nanoparticle volume fraction at two temperatures (*open circle* 303 K, *filled circle* 333 K), and of CuO/EG nanofluid (*open square* 303 K, *filled square* 333 K). *Full lines* represent Eq. (3)

water and CuO/EG nanofluids, with the predictions of Eq. (3). An excellent agreement can be seen.

Conclusions

At present, nanofluid thermal conductivity data and measurement methods lack of consistency. In this paper, the authors have measured thermal conductivities of nanoparticles of CuO dispersed in water and EG, as a function of the particle volume fraction. The temperatures varied between 298 and 338 K. A microcalorimetric technique has been used. It is particularly suitable for studying nanofluids because the measurements are made with very small temperature gradients and with practical absence of natural convection.

Hence, these measurements represent a relevant contribution to the issue of scatter of the nanofluids relative thermal conductivity data found in the literature. In the scarce literature data available, it is shown that the relative thermal conductivity increases. Nevertheless, our results indicate that it is essentially temperature independent. We conclude that the observed growth of the thermal conductivity of our nanofluids with increasing temperature is mainly due to the base fluids—water and EG—rather than to the nanoparticles.

There are very few reliable data on specific heat capacities of water or EG-based CuO nanofluids. Thus, this thermal study has been completed with very precise specific heat capacity measurements of the same nanofluids.

The classical Hamilton–Crosser model properly accounts for the thermal conductivity of the studied

nanofluids. Moreover, assuming that the nanoparticles and the base fluid are in thermal equilibrium, the experimental specific heat capacities of nanofluids are correctly justified by the First Law of Thermodynamics.

Acknowledgements The authors acknowledge Ministerio de Educación y Ciencia (Grant No. CTQ2006-15537-C02/PPQ), Spain, for financial support.

References

1. Das SK, Choi SUS, Yu W, Pradeep T. Nanofluids: science and technology. 1st ed. Hoboken: Wiley; 2007.
2. Yu WH, France DM, Routbort JL, Choi SUS. Review and comparison of nanofluid thermal conductivity and heat transfer enhancements. *Heat Transfer Eng.* 2008;29:432–60.
3. Wen D, Lin G, Vafaei S, Zhang K. Review of nanofluids for heat transfer applications. *Particuology.* 2009;7:141–50.
4. Kakaç S, Pramuanjaroenkij A. Review of convective heat transfer enhancement with nanofluids. *Int J Heat Mass Transf.* 2009;52:3187–96.
5. Li Y, Zhou J, Tung S, Schneider E, Xi S. A review on development of nanofluid preparation and characterization. *Powder Technol.* 2009;196:89–101.
6. Gowda R, Sun H, Wang P, Charmchi M, Gao F, Gu Z, Budhlall B. Effects of particle surface charge, species, concentration, and dispersion method on the thermal conductivity of nanofluids. *Adv Mech Eng.* 2010. doi:10.1155/2010/807610.
7. Özeriç S, Kakaç S, Yazicioğlu AG. Enhanced thermal conductivity of nanofluids: a state-of-the-art review. *Microfluid Nanofluid.* 2010;8:145–70.
8. Wang L, Fan J. Nanofluids research: key issues. *Nanoscale Res Lett.* 2010;5:1241–52.
9. Masoud Hosseini S, Moghadassi AR, Henneke D, Ali E. The thermal conductivities enhancement of mono ethylene glycol and paraffin fluids by adding β -SiC nanoparticles. *J Therm Anal Cal.* 2010;101:113–8.
10. Fan J, Wang L. Review of heat conduction in nanofluids. *J Heat Trans T ASME.* 2011;133(4):040801–2.
11. Xie H, Yu W, Li Y, Chen L. Discussion on the thermal conductivity enhancement of nanofluids. *Nanoscale Res Lett.* 2011;6:124–35.
12. Saidur R, Leong KY, Mohammad HA. A review on applications and challenges of nanofluids. *Renew Sust Energ Rev.* 2011;15:1646–68.
13. Bobbo S, Fedele L, Benetti A, Colla L, Fabrizio M, Pagura C, Barison S. Viscosity of water based SWCNH and TiO₂ nanofluids. *Exp Therm Fluid Sci.* 2012;36:65–71.
14. Singh N, Chand G, Kanagaraj S. Investigation of thermal conductivity and viscosity of carbon nanotubes-ethylene glycol nanofluids. *Heat Transf Eng.* 2012;33(9):821–7.
15. Reddy MCS, Rao VV, Reddy BCM, Sarada SN, Ramesh L. Thermal conductivity measurements of ethylene glycol water based TiO₂ nanofluids. *Nanosci Nanotechnol Lett.* 2012;4(1):105–9.
16. Shanthi R, Anandan SS, Ramalingam V. Heat transfer enhancement using nanofluids: an overview. *Therm Sci.* 2012;16(2):423–44.
17. Mahbulul IM, Saidur R, Amalina MA. Latest developments on the viscosity of nanofluids. *Int J Heat Mass Transf.* 2012;55(4):874–85.

18. Jung JY, Kang YT. Effect of surface charge state on the thermal conductivity of nanofluids. *Heat Mass Transf.* 2012; 48(4):713–8.
19. Yang JC, Li FC, Zhou WW, He YR, Jiang BC. Experimental investigation on the thermal conductivity and shear viscosity of viscoelastic-fluid-based nanofluids. *Int J Heat Mass Transf.* 2012;55(11–12):3160–6.
20. Khedkar RS, Sonawane SS, Wasewar KL. Influence of CuO nanoparticles in enhancing the thermal conductivity of water and monoethylene glycol based nanofluids. *Int Commun Heat Mass.* 2012;39(5):665–9.
21. Kole M, Dey TK. Effect of prolonged ultrasonication on the thermal conductivity of ZnO–ethylene glycol nanofluids. *Thermochim Acta.* 2012;535:58–65.
22. Karthik R, Nagarajan RH, Raja B, Damodharan P. Thermal conductivity of CuO-DI water nanofluids using 3-omega measurement technique in a suspended micro-wire. *Exp Therm Fluid Sci.* 2012;40:1–9.
23. Vajjha RS, Das DK. A review and analysis on influence of temperature and concentration of nanofluids on thermophysical properties, heat transfer and pumping power. *Int J Heat Mass Transf.* 2012;55(15–16):4063–78.
24. Priya KR, Suganthi KS, Rajan KS. Transport properties of ultra-low concentration CuO–water nanofluids containing non-spherical nanoparticles. *Int J Heat Mass Transf.* 2012;55(17–18):4734–43.
25. Fedele L, Colla L, Bobbo S. Viscosity and thermal conductivity measurements of water-based nanofluids containing titanium oxide nanoparticles. *Int J Refrig.* 2012;35(5):1359–66.
26. Hong J, Kim D. Effects of aggregation on the thermal conductivity of alumina/water nanofluids. *Thermochim Acta.* 2012; 542:28–32.
27. Lee GJ, Kim CK, Lee MK, Rhee CK, Kim S, Kim C. Thermal conductivity enhancement of ZnO nanofluid using a one-step physical method. *Thermochim Acta.* 2012;542:24–7.
28. Aladag B, Halefadi S, Doner N, Mare T, Duret S, Estelle P. Experimental investigations of the viscosity of nanofluids at low temperatures. *Appl Energ.* 2012;97:876–80.
29. Colangelo G, Favale E, de Risi A, Laforgia D. Results of experimental investigations on the heat conductivity of nanofluids based on diathermic oil for high temperature applications. *Appl Energ.* 2012;97:828–33.
30. Pang C, Jung JY, Lee JW, Kang YT. Thermal conductivity measurement of methanol-based nanofluids with Al₂O₃ and SiO₂ nanoparticles. *Int J Heat Mass Transf.* 2012;55(21–22):5597–602.
31. Zafarani-Moattar MT, Majdan-Cegincara R. Effect of temperature on volumetric and transport properties of nanofluids containing ZnO nanoparticles poly(ethyleneglycol) and water. *J Chem Thermodyn.* 2012;54:55–67.
32. Tian F, Sun L, Venart JES, Prasad RC, Mojumdar SC. Development of a thermal conductivity cell with nanolayer coating for thermal conductivity measurement of fluids. *J Therm Anal Cal.* 2008;94(1):37–43.
33. Barbés B, Páramo R, Sobrón V, Blanco E, Casanova C. Thermal conductivity measurements of liquids by means of a microcalorimeter. *J Therm Anal Cal.* 2011;104:805–12.
34. Vargaftik AB, Filippov LP, Tarzimanov AA, Totkii EE. Handbook of thermal conductivity of liquids and gases. Boca Raton: CRC Press Inc; 1994.
35. Le Neindre B. Thermal conductivity. In: Marsh KN, editor. Recommended reference materials for the realization of physicochemical properties. Oxford: Blackwell; 1987. p. 321–70.
36. Labudová G, Vozárová V. Uncertainty of the thermal conductivity measurement using the transient hot wire method. *J Therm Anal Cal.* 2002;67:257–65.
37. Buongiorno J, Venerus DC, Prabhat N, McKrell T, Townsend J, Christianson R, Tolmachev YV, Keblinski P, Hu LW, Alvarado JL, Bang IC, Bishnoi SW, Bonetti M, Botz F, Cecere A, Chang Y, Chen G, Chen HS, Chung SJ, Chyu MK, Das SK, Di Paola R, Ding YL, Dubois F, Dzido G, Eapen J, Escher W, Funfschilling D, Galand Q, Gao JW, Gharagozloo PE, Goodson KE, Gutierrez JG, Hong HP, Horton M, Hwang KS, Iorio CS, Jang SP, Jarzebski AB, Jiang YR, Jin LW, Kabelac S, Kamath A, Kedzierski MA, Kieng LG, Kim C, Kim JH, Kim S, Lee SH, Leong KC, Manna I, Michel B, Ni R, Patel HE, Philip J, Poulikakos D, Reynaud C, Savino R, Singh PK, Song PX, Sundararajan T, Timofeeva E, Triticak T, Turanov AN, Van Vaerenbergh S, Wen DS, Witharana S, Yang C, Yeh WH, Zhao WH, Zhou SQ. A benchmark study on the thermal conductivity of nanofluids. *J Appl Phys.* 2009;106:094312.
38. Barbés B, Páramo R, Sobrón V, Blanco E, Pastoriza-Gallego MJ, Piñeiro MM, Legido JL, Casanova C. Thermal conductivity and specific heat capacity measurements of Al₂O₃ nanofluids. *J Therm Anal Cal.* 2013;111(2):1615–25.
39. De Robertis E, Cosme EHH, Neves RS, Kuznetsov AY, Campos APC, Landi SM, Achete CA. Application of the modulated temperature differential scanning calorimetry technique for the determination of the specific heat of copper nanofluids. *Appl Therm Eng.* 2012;41:10–7.
40. O’Hanley H, Buongiorno J, McKrell T, Hu LW. measurement and model Validation of Nanofluid Specific heat capacity with differential scanning calorimetry. *Adv Mech Eng.* 2012;. doi:10.1155/2012/181079.
41. Murshed SMS. Simultaneous measurement of thermal conductivity, thermal diffusivity, and specific heat of nanofluids. *Heat Transf Eng.* 2012;33(8):722–31.
42. Sommers AD, Yerkes KL. Experimental investigation into the convective heat transfer and system-level effects of Al₂O₃-propanol nanofluid. *J Nanopart Res.* 2010;12:1003–14.
43. Nieto de Castro CA, Lourenço MJV, Ribeiro APC, Langa E, Vieira SIC. Thermal properties of ionic liquids and ionanofluids of imidazolium and pyrrolidinium liquids. *J Chem Eng Data.* 2010;55:653–61.
44. Zhou LP, Wang BX, Peng XF, Du XZ, Yang YP. On the specific heat capacity of CuO nanofluid. *Adv Mech Eng.* 2010;. doi:10.1155/2010/172085.
45. Wei C, Nan Z, Wang X, Tan Z. Investigation on thermodynamic properties of a water-based hematite nanofluid. *J Chem Eng Data.* 2010;55:2524–8.
46. Pantzali MN, Kanaris AG, Antoniadis KD, Mouza AA, Paras SV. Effect of nanofluids on the performance of a miniature plate heat exchanger with modulated surface. *Int J Heat Fluid Fl.* 2009;30:691–9.
47. Nan Z, Zhang P, Yu A, Wei C, Shi Q, Tan Z. Novel synthesis of β-FeOOH nanofluid and determination of its heat capacity by an adiabatic calorimeter. *Chinese J Chem.* 2009;27:1249–53.
48. Vajjha RS, Das DK. Specific heat measurement of three nanofluids and development of new correlations. *J Heat Trans T ASME.* 2009;131(7):071601.
49. Nelson IC, Banerjee D, Ponnappan R. Flow loop experiments using polyalphaolephin nanofluids. *J Thermophys Heat Trans.* 2009;23(4):752–61.
50. Zhou SQ, Ni R. Measurement of the specific heat capacity of water-based Al₂O₃ nanofluid. *App Phys Lett.* 2008;92:093123.
51. Amrollahi A, Hamidi AA, Rashidi AM. The effects of temperature, volume fraction and vibration time on the thermo-physical properties of a carbon nanotube suspension (carbon nanofluid). *Nanotechnology.* 2008;19:315701.
52. Kulkarni DP, Vajjha RS, Das DK, Oliva D. Application of aluminium oxide nanofluids in diesel electric generator as jacket water coolant. *App Therm Eng.* 2008;28:1774–81.

53. Barbés B, Blanco E, Casanova C, Páramo R. A temperature-dependent model for the measurement of the thermal conductivity of liquids, using a microcalorimeter. *Meas Sci Technol*. 2011;22:045401.
54. Ramires MLV, Nieto de Castro CA, Nagasaka Y, Nagashima A, Assael MJ, Wakeham WA. Standard reference data for the thermal conductivity of water. *J Phys Chem Ref Data*. 1995;24(3):1377–81.
55. Assael MJ, Charitidou E, Nieto de Castro CA, Wakeham WA. The thermal conductivity of n-hexane, n-heptane and n-decane by the transient hot-wire method. *Int J Thermophys*. 1987;8(6):663–70.
56. Páramo R, Zouine M, Sobrón F, Casanova C. Saturated heat capacities of some linear and branched alkyl-benzenes between 288 and 348 K. *Int J Thermophys*. 2003;24(1):185–99.
57. Lee S, Choi SUS, Li S, Eastman JA. Measuring thermal conductivity of fluids containing oxide nanoparticles. *Trans ASME*. 1999;121:280–9.
58. Eastman JA, Choi SUS, Li S, Soyez G, Thompson LJ, DiMelfi RJ. Novel thermal properties of nanostructured materials. *Mat Sci Forum*. 1999;312–314:629–34.
59. Das SK, Putra N, Thiesen P, Roetzel W. Temperature dependence of thermal conductivity enhancement for nanofluids. *J Heat Transf*. 2003;125:567–74.
60. Patel HE, Sundararajan T, Das SK. An experimental investigation into the thermal conductivity enhancement in oxide and metallic nanofluids. *J Nanopart Res*. 2010;12:1015–31.
61. Zhang Z, Gu H, Fujii M. Effective thermal conductivity and thermal diffusivity of nanofluids containing spherical and cylindrical nanoparticles. *Exp Therm Fluid Sci*. 2007;31:593–9.
62. Mints HA, Roy G, Nguyen CT, Doucet D. New temperature dependent thermal conductivity data for water based nanofluids. *Int J Therm Sci*. 2009;48:363–71.
63. Hwang Y, Park HS, Lee JK, Jung WH. Thermal conductivity and lubrication characteristics of nanofluids. *Curr Appl Phys*. 2006;6S1:e67–71.
64. Wang X, Su X, Choi SUS. Thermal conductivity of nanoparticle-fluid mixture. *J Thermophys Heat Transf*. 1999;13(4):474–80.
65. Timofeeva EV, Gavrilov AN, McCloskey JM, Tolmachev YV, Sprunt S, Lopatina LM, Selinger JV. Thermal conductivity and particle agglomeration in alumina nanofluids: experiment and theory. *Phys Rev E*. 2007;76:061203.
66. Hamilton RL, Crosser OK. Thermal conductivity of heterogeneous two component systems. *Ind Eng Chem Fundam*. 1962;1:187–91.
67. Maxwell JC. A treatise on electricity and magnetism. Oxford: Clarendon; 1891.
68. Nan CW, Birringer R, Clarke DR, Gleiter H. Effective thermal conductivity of particulate composites with interfacial thermal resistance. *J Appl Phys*. 1997;81:6692–9.
69. Jang SP, Choi SUS. Role of Brownian motion in the enhanced thermal conductivity of nanofluids. *Appl Phys Lett*. 2004;84:4316–8.
70. Eapen J, Rusconi R, Piazza R, Yip S. The classical nature of thermal conduction in nanofluids. *J Heat Trans T ASME*. 2010;132(10):102402.